nature cell biology

Wnt activity defines colon cancer stem cells and is regulated by the microenvironment

Louis Vermeulen[1,5], Felipe De Sousa E Melo[1,5], Maartje van der Heijden[1], Kate Cameron[1], Joan H. de Jong[1], Tijana Borovski[1], Jurriaan B. Tuynman[1], Matilde Todaro[2], Christian Merz[3], Hans Rodermond[1], Martin R. Sprick[1], Kristel Kemper[1], Dick J. Richel[1], Giorgio Stassi[2,4] and Jan Paul Medema[1,6].

Despite the presence of mutations in APC or β-catenin, which are believed to activate the Wnt signalling cascade constitutively, most colorectal cancers show cellular heterogeneity when β-catenin localization is analysed, indicating a more complex regulation of Wnt signalling. We explored this heterogeneity with a Wnt reporter construct and observed that high Wnt activity functionally designates the colon cancer stem cell (CSC) population. In adenocarcinomas, high activity of the Wnt pathway is observed preferentially in tumour cells located close to stromal myofibroblasts, indicating that Wnt activity and cancer stemness may be regulated by extrinsic cues. In agreement with this notion, myofibroblast-secreted factors, specifically hepatocyte growth factor, activate β-catenin-dependent transcription and subsequently CSC clonogenicity. More significantly, myofibroblast-secreted factors also restore the CSC phenotype in more differentiated tumour cells both *in vitro* and *in vivo*. We therefore propose that stemness of colon cancer cells is in part orchestrated by the microenvironment and is a much more dynamic quality than previously expected that can be defined by high Wnt activity.

The sequential events driving the transition of normal colonic mucosa to adenocarcinoma have been well documented and depend critically on alterations to Wnt signalling[1–4]. In normal cells the transcriptional regulator β-catenin is tightly controlled by a multiprotein complex that contains the tumour suppressor adenomatous polyposis coli (APC)[2]. Activation of Frizzled receptors by Wnt ligands disrupts this complex and results in the translocation of β-catenin to the nucleus, where it associates with the T-cell factor/lymphoid enhancer factor (TCF/LEF) family of transcription factors to activate specific Wnt target genes[5,6]. Under physiological conditions, Wnt activity is crucial for intestinal stem cells and crypt homeostasis[7]. However, Wnt signalling also has a central function in pathological settings[2]. Mutation of APC or β-catenin is an early event in the transformation of colonic epithelial cells, but established colorectal cancers also depend critically on Wnt signalling[8]. APC mutations generally result in a defective β-catenin degradation complex and, as a consequence, the accumulation of β-catenin in the nucleus and the perpetual transcription of Wnt target genes[9]. Although this would imply that all tumour cells contain active Wnt signalling, immunohistochemical studies have revealed that colon carcinomas harbouring APC mutations do not contain nuclear β-catenin homogeneously (Fig. 1a)[10,11]. This so-called β-catenin paradox is intriguing in the light of recent observations that indicate that only a subset of tumour cells, CSCs, are endowed with tumorigenic capacity[12], whereas most tumour cells have undergone differentiation and lost their tumorigenic potential. CSCs have been identified by using several markers, such as CD133 and CD166 (refs 13–16). Because Wnt signalling is a dominant force preserving the normal fate of colon stem cells[2], we proposed a preponderant role for this pathway in colon CSCs as well.

Using a TCF/LEF reporter that directs the expression of enhanced green fluorescent protein (TOP–GFP) we provide evidence that Wnt signalling activity is a marker for colon CSCs and is regulated by the microenvironment. Moreover, we show that differentiated cancer cells, which have lost the capacity to form tumours and are no longer clonogenic, can be reprogrammed to express CSC markers and regain their tumorigenic capacity when stimulated with myofibroblast-derived factors. This suggests that cancer stemness is not a rigid feature but can be modulated and even installed by the microenvironment.

RESULTS

Colon cancer spheroidal cultures have heterogeneous Wnt activity levels

Primary spheroidal cultures of colon cancer cells consist of cells expressing CSC markers and on injection induce a tumour that closely

[1]Laboratory for Experimental Oncology and Radiobiology (LEXOR), Center for Experimental Molecular Medicine (CEMM), Academic Medical Center (AMC), University of Amsterdam, 1105 AZ Amsterdam, The Netherlands. [2]Department of Surgical and Oncological Sciences, Cellular and Molecular Pathophysiology Laboratory, University of Palermo, 90127 Palermo, Italy. [3]APOGENIX GmbH, 69120 Heidelberg, Germany. [4]Present address: Cellular and Molecular Oncology, IRCCS Fondazione Salvatore Maugeri, 27100 Pavia, Italy.
[5]These authors contributed equally to this work.
[6]Correspondence should be addressed to J.P.M. (J.P.Medema@amc.uva.nl)

Received 22 January 2010; accepted 26 March 2010; published online 25 April 2010; DOI:10.1038/ncb2048

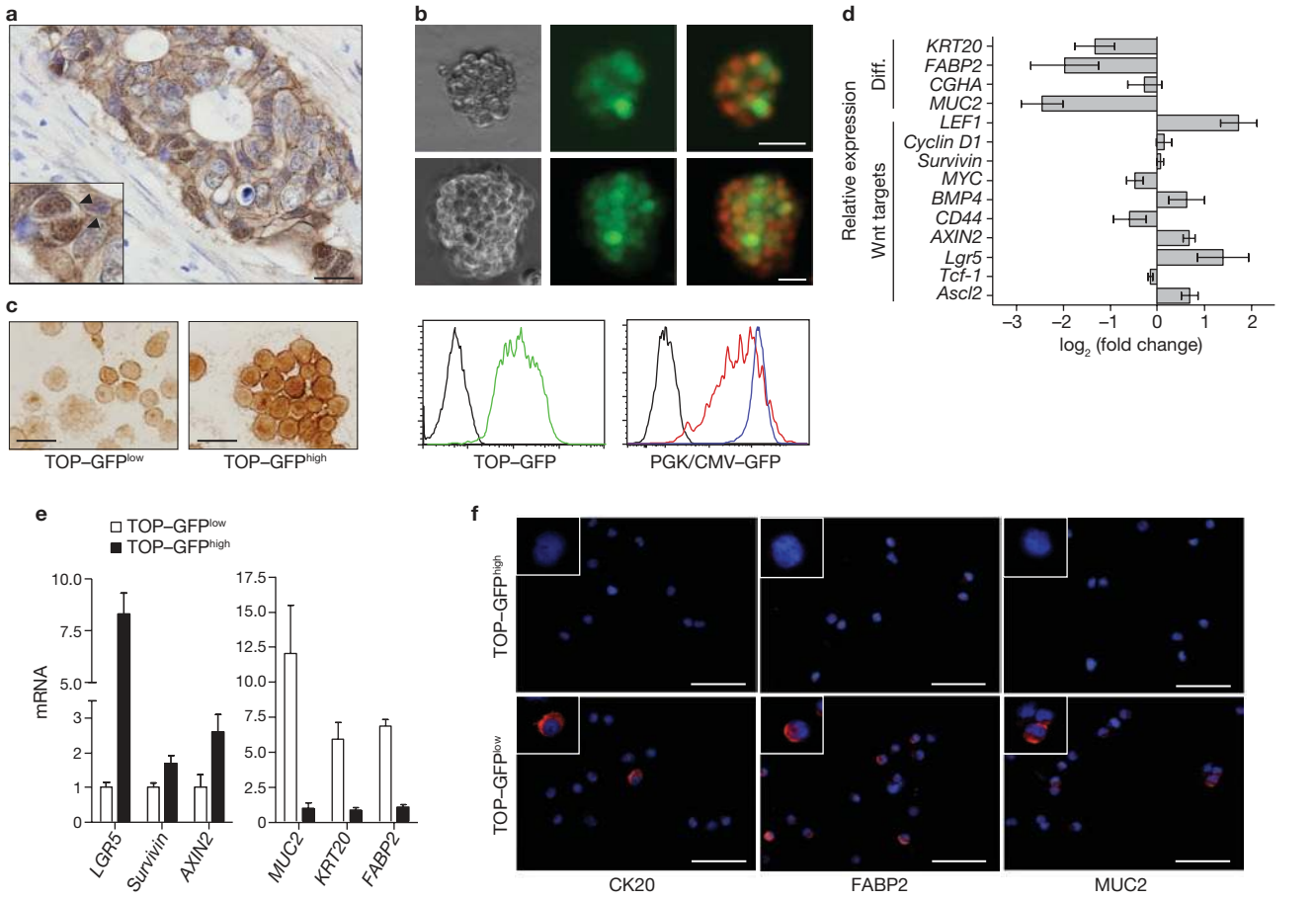

Figure 1 Wnt heterogeneity in primary tumours and in CSC culture. (**a**) Colorectal cancer patient material stained for β-catenin. Scale bar, 20 μm. (**b**) The top two rows show two separate single-cell-cloned colon CSC cultures, lentivirally transduced with TOP–GFP[18], revealed by phase contrast (left) and fluorescence microscopy (middle). Nuclei were counterstained with 4,6-diamidino-2-phenylindole (red, right). Scale bars, 20 μm. Bottom two panels: fluorescence-activated cell sorting (FACS) profile of GFP intensity range for a single-cell-cloned TOP–GFP-carrying colon CSC culture (green line, left) compared with the sharp range of GFP in the CMV–GFP (blue line, right) culture and non-single-cell-cloned PGK–GFP-transduced culture (red line, right). Non-transduced parental culture was used as a control for GFP background intensity (black lines). (**c**) Cytospins of the highest and lowest 10% TOP–GFP fractions stained for β-catenin. Scale bars, 20 μm. (**d**) Microarray analysis was performed on the highest and lowest 10% TOP–GFP fractions. The $\log_2$ fold change in gene expression between the TOP–GFP^{high} and TOP–GFP^{low} fraction is shown. Each bar represents the average fold change of three different single-cell-cloned TOP–GFP cultures. Several Wnt target genes are listed and their expression is correlated with the TOP–GFP^{high} fraction. Genes associated with differentiation (Diff.) are upregulated in the TOP–GFP^{low} fraction. Error bars represent s.e.m. for four different data sets from three different cultures. (**e**) Differential expression of several Wnt target genes (left) and differentiation markers (right) between TOP–GFP^{high} and TOP–GFP^{low} fractions validated by qPCR. Error bars represent s.d. ($n = 3$). (**f**) Cytospins of sorted TOP–GFP^{high} and TOP–GFP^{low} cells stained for differentiation markers as indicated. Scale bars, 80 μm.

resembles the original human malignancy[17]. To investigate the relation of the β-catenin paradox (Fig. 1a) with the CSC phenotype, we assessed Wnt signalling activity in these colon CSC cultures with a TOP–GFP reporter or with control reporters, phosphoglycerate kinase (PGK)–GFP or cytomegalovirus (CMV)–GFP[18]. To exclude variation in lentiviral integration site and copy number between cells, the transduced culture was single-cell cloned, a procedure that preserves all characteristics of the spheroidal culture[17]. Strikingly, cells in these single-cell-derived TOP–GFP cultures still showed considerable heterogeneity in Wnt signalling levels (about 100-fold) (Fig. 1b). These expression differences were not observed when a constitutively active CMV promoter was used to drive GFP expression (Fig. 1b), indicating that heterogeneity is due to differences in β-catenin-driven transcription even though that these cells carry an APC mutation. In agreement with this notion, the variation in TOP–GFP levels was accompanied by heterogeneity in nuclear β-catenin localization (Fig. 1c; Supplementary Information, Fig. S1a, b). Moreover, microarray analysis on the highest and lowest 10% of TOP–GFP-expressing cells revealed that stem-cell-associated Wnt target genes, including those encoding the intestinal stem cell markers LGR5 (leucine-rich repeat-containing G protein-coupled receptor 5) and ASCL2 (achaete-scute-like 2) (refs 19, 20), were predominantly upregulated in the TOP–GFP^{high} fraction, whereas genes associated with epithelial differentiation (those encoding mucin 2, *MUC2*; cytokeratin 20, *KRT20* and fatty-acid binding protein 2, *FABP2*) were clearly enhanced in the TOP–GFP^{low} fraction (Fig. 1d; see Supplementary Information, Table S1, for a list of the most significant genes). Expression of differentiation-associated genes in TOP–GFP^{low} was confirmed by quantitative PCR (qPCR) as well as at the protein level (Fig. 1e, f). Taken together, these results indicates that spheroidal CSC cultures contain heterogeneity in Wnt signalling activity, which is inversely correlated with heterogeneity in differentiation markers.

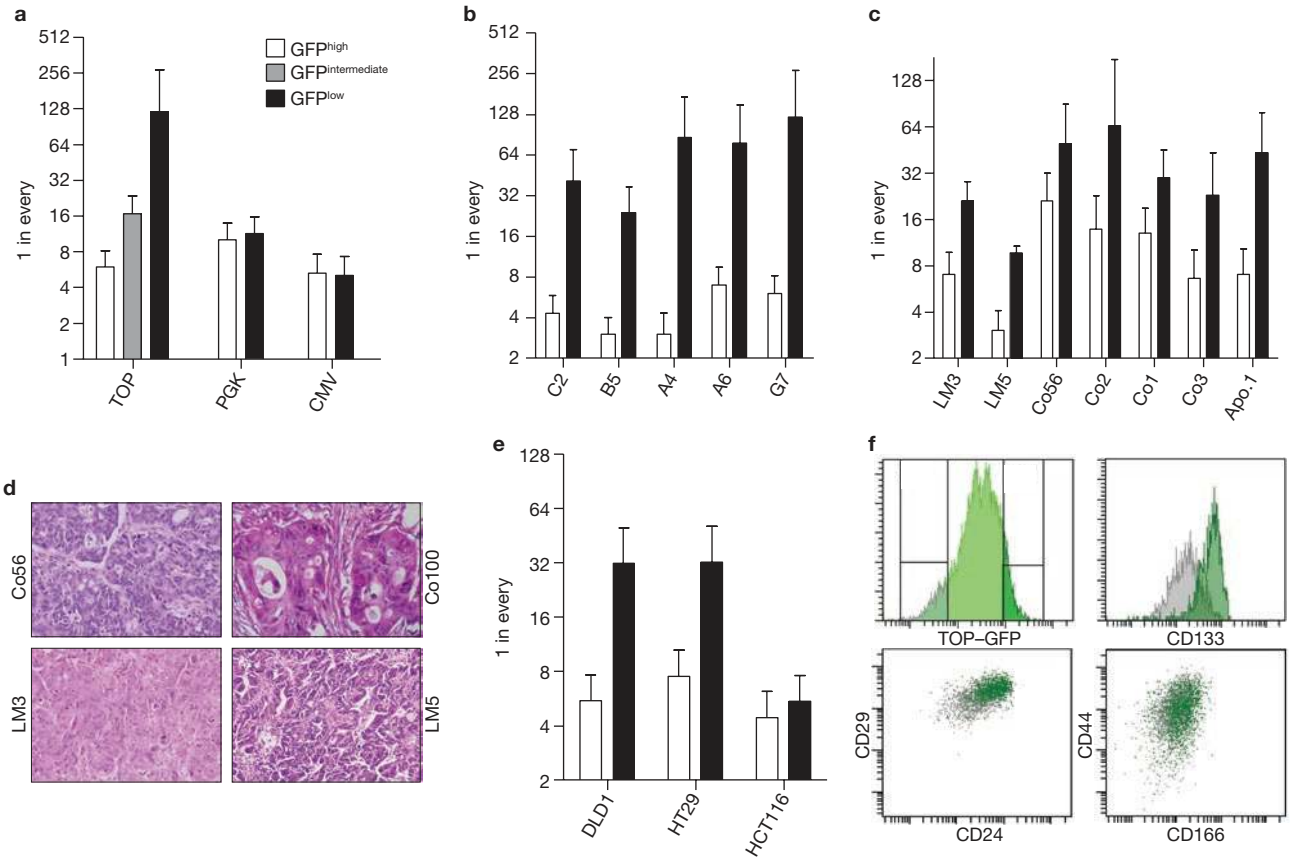

Figure 2 Cells with high Wnt signalling show CSC properties *in vitro*. (**a**) A limiting dilution was performed on the high, intermediate and low TOP–GFP cell fractions. The graph presents the clonogenic potential of each cell fraction. As a control a CMV–GFP single-cell-derived culture and a non-single-cell-derived PGK–GFP culture are depicted. GFP^{high}, $GFP^{intermediate}$ and GFP^{low} represent the highest, middle and lowest 10% cell fractions, respectively. See Methods for details on limiting-dilution statistics and scheme. (**b**) Limiting-dilution assay and clonogenic potential of the five independent single-cell-derived clones from line Co100. (**c**) Limiting-dilution assay and clonogenic potential of the highest and lowest 10% TOP–GFP levels of a series of TOP–GFP-expressing CSC lines (non-single-cell-cloned). (**d**) A panel of haematoxylin/eosin stainings of the corresponding primary colon cancers used to generate the spheroidal cultures in **a**–**c**. (**e**) Limiting-dilution assay and clonogenic potential of the highest and lowest 10% TOP–GFP levels of three established colon cancer cell lines. **b**, **c** and **e**, white bars represent highest 10% TOP–GFP cells and black bars represent lowest 10% TOP–GFP cells. Error bars in **a**–**c** and **e** represent 95% confidence intervals. See Methods for details on limiting dilution statistics and scheme. (**f**) TOP–GFP levels are associated with CSC marker expression. CD133 correlates with TOP–GFP^{high} intensity. The combination of CD24/CD29 or CD44/CD166 also shows a correlation with the TOP–GFP^{high} fraction.

Colon CSCs are characterized by high expression levels of Wnt

The variation in TOP–GFP levels not only determined gene-expression differences; it also had significant biological consequences. In the TOP–GFP^{high} fraction, clonogenic potential was superior to that of TOP–GFP^{low} cells, whereas differential clonogenicity was not observed in cultures expressing GFP driven by constitutive promoters (Fig. 2a). Intermediate TOP–GFP-expressing cells had intermediate clonogenicity and intermediate gene-expression profiles (Fig. 2a; Supplementary Information, Fig. S1c), suggesting that Wnt signalling activity could serve as a functional marker for tumour cell clonogenicity and cancer stemness. Indeed, TOP–GFP-based segregation of clonogenicity is a common principle and was observed with separate single-cell-derived clones of the same CSC line (Fig. 2b) as well as in a series of other primary colon spheroidal cultures or several established human colon cancer cell lines (Fig. 2c–e; Supplementary Information, Fig. S2a). These separate spheroidal cultures and cell lines were not cloned from a single cell, which excludes the possibility of clonal artefacts but also limits the segregation of clonogenicity as a result of differences between cells in lentiviral integration. Mutation analysis of the different lines indicated that Wnt signalling heterogeneity and its effect on clonogenicity seems to be independent of the mutation status of p53 (compare Co100; wild-type, WT, p53, for example) with LM5 (mutant p53)) or K-Ras (compare Co100; mutant K-Ras with LM5; WT K-Ras, for example), or microsatellite stability (compare Co56, DLD-1; microsatellite unstable with Co100 and LM5; microsatellite stable, for example). The only striking exception is the HCT-116 cell line, which contains a β-catenin mutation. Whether this is a consistent finding for β-catenin mutant lines remains to be established, but recent findings have pointed out that HCT-116 is not organized in a hierarchical fashion and may therefore not contain a more clonogenic CSC fraction[21,22]. We therefore propose that the activity of the Wnt pathway defines a hierarchical divergence of CSCs and their differentiated progeny in colorectal cancer. This is supported by the finding that Wnt activity levels correlate with the surface expression of previously applied markers for colon CSCs (Fig. 2f).

CSCs are defined by their ability to induce tumours that closely resemble the original malignancy on injection into immune-deficient mice[23]. We reported previously that spheroidal cultured colon cancer cells fulfilled these criteria and therefore contain CSCs[14,17]. Injection of

a

Fraction	Cells injected			
	10	100	1,000	5,000
Total	1/6	6/6	6/6	–
TOP–GFP^{low}	0/6	0/6	1/6	3/6
TOP–GFP^{intermediate}	4/6	5/6	4/6	–
TOP–GFP^{high}	3/6	5/6	6/6	–

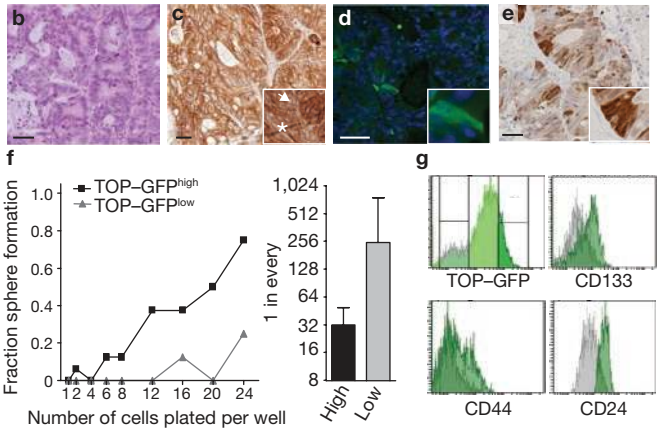

Figure 3 Cells with high Wnt signalling show CSC properties *in vivo*. (**a**) *In vivo* transfer of TOP–GFP-transduced cultures. Cell numbers from the indicated populations were injected into nude mice after FACS. The number of successful tumour initiations after nine weeks out of six injections for each condition is shown. The TOP–GFP^{high} fraction showed the highest tumour-initiating capacity. (**b**) Haematoxylin/eosin staining of xenografts shows clear evidence of colon carcinoma morphology. (**c**) Xenografts show heterogeneous nuclear β-catenin (arrow); the asterisk indicates a region without nuclear localization. (**d**, **e**) Immunofluorescence (**d**) and immunohistochemistry (**e**) for GFP show clear heterogeneous TOP–GFP levels. Scale bars in **b**–**e**, 50 μm. (**f**) TOP–GFP xenografts were dissociated, tumour cells from the TOP–GFP^{high} and TOP–GFP^{low} fractions were plated for limiting dilutions and the clonogenic potential was determined. Error bars represent 95% confidence intervals. A representative example of two independent experiments is shown. (**g**) Correlation of CSC markers and TOP–GFP levels is also seen in freshly dissociated xenografts.

a

Fraction	Cells injected			
	1	10	100	1,000
Total	ND	0/6	1/6	2/6
TOP–GFP^{low}	ND	0/6	1/6	0/6
TOP–GFP^{high}	1/4	3/6	2/6	5/6

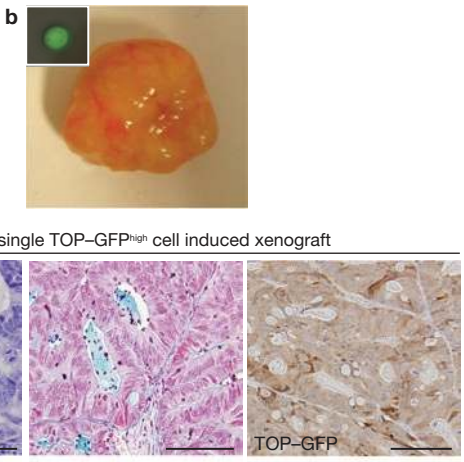

Figure 4 *Ex vivo* tumorigenic assay and single-cell-derived tumours. (**a**) TOP–GFP xenografts were dissociated and subcutaneously injected to determine their tumorigenicity and thus their self-renewal capacity. Cell numbers from indicated populations were injected into nude mice after FACS. The number of successful tumour initiations after nine weeks out of six injections for each condition is shown. The TOP–GFP^{high} fraction showed the highest tumour-initiating capacity. The total population was used as a control. Note that one single TOP–GFP^{high} cell initiated a tumour out of four implants (see Methods for details). ND, none detected. (**b**) Xenotransplanted tumour derived from a single TOP–GFP^{high} cell sorted directly *ex vivo*. The inset shows a single cell; the figure shows an isolated xenotransplant. (**c**) Haematoxylin/eosin staining (left), Alcian Blue staining (middle) and anti-GFP immunohistochemistry (right) of the single-cell-derived tumour. Scale bars, 100 μm.

TOP–GFP cells into nude mice confirmed that CSCs can be identified through their Wnt signalling activity, because the TOP–GFP^{high} fraction was much more effective in inducing tumours on injection into mice (Fig. 3a). A similar segregation was observed when TOP–GFP^{high} cells (3 of 6 injections yielded tumours when 100 cells injected) and TOP–GFP^{low} cells (0 of 6 injections yielded tumours) were injected into fully immunodeficient NOD/SCID (non-obese diabetic/severe combined immunodeficiency) IL-2 receptor gamma chain null (*Il2rg*$^{-/-}$) mice, suggesting that the TOP–GFP^{high} definition of CSCs is independent of a remnant immune response. More significantly, xenografts derived from TOP–GFP-transduced spheroidal cultures closely recapitulated the original malignancy (Figs 2d and 3b) but also showed a heterogeneous distribution of cells containing nuclear β-catenin and TOP–GFP activity (Fig. 3c–e). The TOP–GFP^{high} fraction *in vivo* contained both cycling and non-cycling cells, as demonstrated by co-staining for Ki-67 (Supplementary Information, Fig. S2b). We consider this as strong evidence for the maintained regulation of Wnt signalling in clonal populations of colorectal cancer cells *in vivo*, which is in line with the β-catenin paradox[10,11]. Consistent with the idea that the clonogenic CSC potential resides in the 'Wnt-high' population, we found that *in vitro* outgrowth of cells isolated from such TOP–GFP-expressing xenografts is much more effective with TOP–GFP^{high} cells than in TOP–GFP^{low} cells (Fig. 3f). Moreover, we also observed a strong correlation between TOP–GFP activity and previously used colon CSC markers[17] in *ex vivo*-derived cells (Fig. 3g).

To prove formally that TOP–GFP^{high} cells are CSCs and have self-renewal capacity, we performed direct *in vivo* transfer of xenograft-derived cells with a limiting dilution of the 10% highest, lowest and unselected TOP–GFP cells. Whereas TOP–GFP^{high} cells induced tumour growth effectively on transfer, TOP–GFP^{low} cells largely failed to do so (Fig. 4a). Using Wnt activity as a CSC marker, we even managed to generate colon cancer xenografts starting from either one *ex vivo*-derived TOP–GFP^{high} cell (1 of 4 injected) (Fig. 4b) or from one spheroidal-culture-derived TOP–GFP^{high} cell (8 of 50 injected). The resulting tumours again resembled the original malignancy in differentiation and also showed clear heterogeneity in TOP–GFP (Fig. 4c). Taken together, these results illustrate that a subfraction of colon tumour cells are endowed with tumorigenic potential, which can be identified on the basis of Wnt activity. At the same time, these data point to Wnt regulatory mechanisms in colorectal cancer cells even in the presence of APC mutations.

Myofibroblast-secreted factors enhance Wnt signalling activity in colon cancer cells

Having established that TCF/LEF-driven transcription is regulated in colorectal cancer and is an important determinant for CSC features, we wished to understand the mechanisms underlying this regulation. It

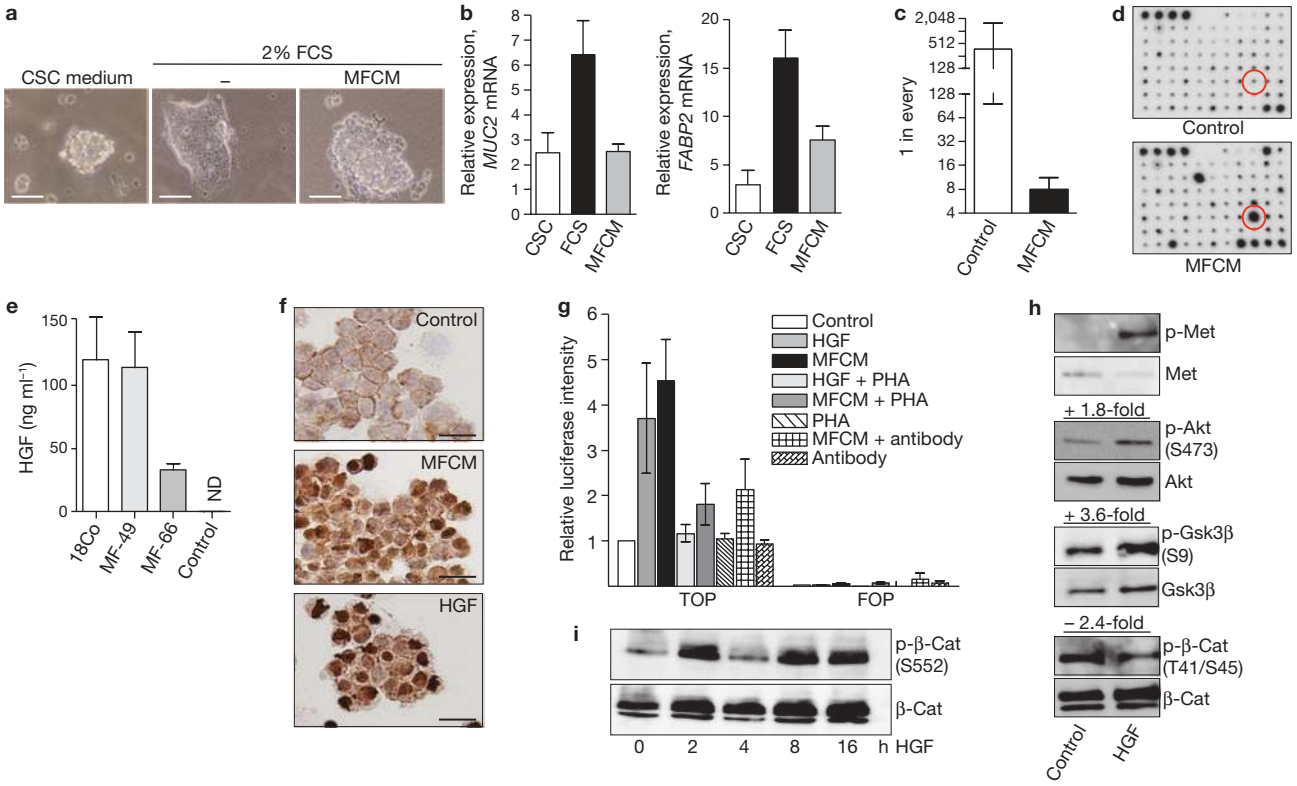

Figure 5 Myofibroblasts support stem-cell properties and regulate Wnt signalling. (**a**) Colon CSC cultures (left) can be differentiated by plating the cells on tissue-culture-treated plastic plates in medium containing serum (middle). Serum-induced morphological differentiation is prevented in the presence of MFCM derived from the colonic cell line 18Co (right). Scale bar, 20 μm. (**b**) Expression of differentiation genes Muc2 and FABP2 as determined by qPCR in CSCs and in cells induced to differentiate in the absence or presence of MFCM as in **a**. Error bars represent s.d. ($n = 3$). (**c**) Clonogenic potential determined by limiting-dilution assays in the presence or absence of MFCM. Error bars represent 95% confidence intervals. A representative example is shown. (**d**) Cytokine array detecting a panel of 79 cytokines. Analysis of MFCM reveals a high level of HGF production (red circle). (**e**) HGF production detected by enzyme-linked immunosorbent assay in MFCM and in two primary cell lines (CRC-MF49 and CRC-MF66) isolated from colorectal cancer patients. Error bars represent s.d. ($n = 3$). ND, none detectable. (**f**) Treatment of CSC cultures with MFCM or HGF for 4 h induces nuclear translocation of β-catenin. Scale bars, 20 μm. (**g**) Treatment of CSC cultures with MFCM or HGF for 16 h activates TOP–luciferase reporter activity, which is prevented by PHA or specific anti-HGF neutralizing antibodies. Error bars represent s.e.m. ($n = 3$); the experiment shown is representative of three independent experiments. (**h**) Western blot of c-Met, PKB/Akt, GSK3β and T41/S45 β-catenin with normal or phospho-specific antibodies with and without stimulation with 50 ng ml^{-1} HGF for 2 h. Numbers indicate the fold induction or decrease as determined by total and phospho-specific signals. (**i**) Total amount of β-catenin and S552 phosphorylated β-catenin over time after stimulation with HGF. Uncropped images of blots in **h** and **i** are shown in Supplementary Information, Fig. S7.

was apparent from our spheroidal cultures that part of the regulation is a tumour-cell-intrinsic feature, because single CSCs quickly reformed cultures with heterogeneous Wnt activity. Nevertheless, *in vivo* observations suggest that extrinsic factors may also be instrumental in directing Wnt activity in colorectal cancer[10,11]. Different cell types recruited and/or activated within the tumour could participate in shaping and organizing this heterogeneity. This external control emerges as a sustainable force in malignancy progression[24]. Strikingly, normal intestinal stem cells have also recently been shown to have cell-autonomous regulation of Wnt activity[25], although extrinsic cues emanating from cells within or surrounding the crypt also contribute to normal epithelial stem cell function[26]. In colorectal cancer, the β-catenin paradox has indirectly implicated the stroma, of which myofibroblasts are an important component (Supplementary Information, Fig. S3a), as a potential regulator of Wnt signalling[10,11]. To directly address whether myofibroblasts could affect Wnt signalling we analysed co-cultures of myofibroblasts and CSCs. We have previously shown that colon CSCs differentiate and lose CSC markers in serum-containing medium[14,17]. However, when CSCs were co-cultured with a colonic myofibroblast cell line or even in the presence of conditioned medium derived from such myofibroblasts (MFCM), morphological and molecular differentiation was prevented (Fig. 5a, b; Supplementary Information, Fig. S3b, c). We also observed a strong functional effect of MFCM on tumour cell clonogenicity, which was markedly changed when CSCs were incubated in the presence or absence of MFCM (more than 50-fold; Fig. 5c). Consistent with the fact that Wnt activity is correlated with clonogenicity, stimulation with MFCM strongly increased nuclear β-catenin localization and Wnt reporter activity (Fig. 5f, g), which shows that myofibroblasts secrete factors regulating Wnt activity and thereby clonogenic capacity.

In an effort to define the growth factors involved in this crosstalk, a cytokine antibody array was performed on MFCM, which revealed hepatocyte growth factor (HGF) as one of the abundant factors present in MFCM (Fig. 5d; Supplementary Information, Fig. S4a). In agreement, a significant amount of HGF was also secreted by myofibroblasts derived from samples from primary colon cancer (Fig. 5e). HGF has been suggested to have a role in colorectal cancer, and its receptor HGFR/c-Met is associated with both Wnt signalling activity[27–29] and colorectal

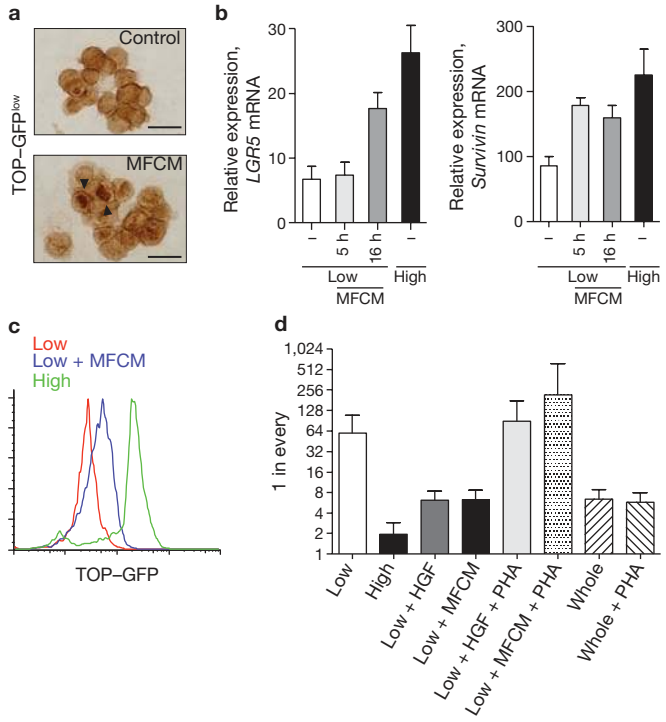

Figure 6 Myofibroblasts restore Wnt activity and clonogenic potential in TOP–GFP^{low} cells. (**a**) Stimulation of TOP–GFP^{low}-sorted cells with MFCM for 4 h induces nuclear translocation of β-catenin. Scale bars, 20 μm. (**b**) Induction of Lgr5 and Survivin as determined by qPCR after 5 and 16 h in TOP–GFP^{low} cells after treatment with MFCM. Error bars represent s.d. ($n = 3$). (**c**) TOP–GFP expression after 16 h in TOP–GFP^{low} cells after treatment with MFCM. (**d**) Limiting-dilution assay to determine the clonogenicity of TOP–GFP^{high}, TOP–GFP^{intermediate} and TOP–GFP^{low} cells. Clonogenicity can be restored in TOP–GFP^{low} cells with HGF or MFCM, whereas phytohaemagglutinin (PHA) blocks this effect yet has no effect on normal clonogenicity. Error bars represent 95% confidence intervals. See Methods for details on limiting-dilution statistics and scheme.

cancer progression[30]. In addition, our CSC cultures expressed c-Met (Supplementary Information, Fig. S4b), and stimulation with HGF or MFCM rapidly activated receptor tyrosine phosphorylation (Fig. 5h; Supplementary Information, Fig. S4c). It is not fully understood how HGF modulates Wnt signalling activity, but we clearly observed an increase in phosphorylation of protein kinase B (PKB)/Akt and glycogen synthase kinase 3β (GSK3β), the latter being associated with diminished GSK3β activity (Fig. 5h). Although the crosstalk between PKB/Akt and the APC complex is a matter of debate[31], in spheroidal cultures of primary colon cancer the stimulation of hepatocyte growth factor decreased the phosphorylation of Thr 41 and Ser 45 in β-catenin (Fig. 5h), which are important regulatory sites for proteasomal degradation of the transcription factor. It remains to be established whether this is a direct effect, but β-catenin stability was induced by HGF (about fourfold at 16 h; Fig. 5i). Moreover, a concomitant increase in phosphorylation of β-catenin on Ser 552, which is associated with enhanced transcription[32], is also detected at an early stage (Fig. 5h, i). The stimulatory effect of both MFCM and HGF on TCF/LEF transcriptional activity was inhibited with a specific c-Met inhibitor (PHA665752) and also with an HGF-blocking antibody (Fig. 5g; Supplementary Information, Fig. S5). We therefore conclude that HGF secreted by myofibroblasts is modulating nuclear β-catenin activity through c-Met and thereby affects CSC features in colorectal tumour cells.

Myofibroblast-secreted factors install a CSC phenotype in differentiated cancer cells

The present observations support a model in which myofibroblasts create what can tentatively be called a CSC niche. By analogy with normal stem cells, distance from the niche then determines the level of stemness-stimulating factors and thereby differentiation, assuming that CSCs follow a unidirectional differentiation pattern and cannot regain CSC features when they have undergone differentiation. However, in contrast to this proposition we observed that HGF-induced β-catenin modulation is a dominant effect of myofibroblasts and can revert differentiation. Treatment of TOP–GFP^{low} cells, which have low levels of nuclear β-catenin and have lost their clonogenic potential (Figs 1c and 2a), with MFCM induced nuclear β-catenin localization as early as 4 h afterwards (Fig. 6a). More significantly, exposure of TOP–GFP^{low} cells to MFCM induced the re-expression of CSC markers (Fig. 6b) and β-catenin-dependent transcription (Fig. 6c) and even restored the clonogenic potential of this population (Fig. 6d). This effect of HGF is a rapid modulation of the TOP–GFP^{low} cells that occurs within 16 h and enhances the clonogenicity by about 5–10-fold, almost to the level of TOP–GFP^{high} cells. This excluded the selective expansion of a small population of CSCs remaining within the TOP–GFP^{low} cells because the doubling time was more than 24 h, thus showing that myofibroblast-secreted factors enhance Wnt signalling and can reinstall features of stemness in more differentiated tumour cells.

The relevance of our findings for Wnt activity *in vivo* and CSC maintenance are supported by the observation that TOP–GFP^{high} cells were preferentially located close to myofibroblasts in xenografts (Fig. 7a). In addition, in samples of primary colon cancer we observed a clear co-localization between cells expressing α-smooth muscle actin (α-SMA) and tumour cells displaying nuclear β-catenin (white arrows in Fig. 7b). This observation was corroborated by co-immunofluorescence of xenotransplanted tumours, which confirmed the correlation between the position of myofibroblasts and the activity of Wnt signalling in the neighbouring tumour cells (Fig. 7c, d). In addition, in primary tumours a role for myofibroblast-derived HGF in Wnt regulation was suggested, because we observed clear expression of HGF in tumour-associated myofibroblasts in most cases (Supplementary Information, Fig. S6a) and, as shown above, significant amounts of HGF production by myofibroblasts isolated from primary colon cancer samples (Fig. 5e; Supplementary Information, Fig. S6b,c). To establish formally that myofibroblasts can reinstall the tumour-initiating capacity in TOP–GFP^{low} cells, we performed co-injections. This revealed that TOP–GFP^{low} cells, which have a very limited capacity to induce tumours in comparison with TOP–GFP^{high} cells, regained tumorigenicity and thus CSC features when co-injected with myofibroblasts or with an admixture of the factors that these cells secrete (MFCM) and Matrigel (Fig. 7e). Our data therefore provide clear evidence of a role for myofibroblasts in installing and maintaining colon CSC fate through the regulation of Wnt signalling.

DISCUSSION

Wnt signalling is crucially important in maintaining stemness in normal colon stem cells and is a common pathway that is deregulated in most colon cancers. Using Wnt signalling activity as a readout, we have unravelled a fundamental characteristic of cancer stemness. In a similar manner to normal intestinal stem cells[26], Wnt activity is not merely a

cell-intrinsic feature that can be used to define CSCs in a series of colon tumours carrying a variety of mutations, but it is also regulated by extrinsic factors. More significantly, our data show that cells surrounding the CSC not only maintain a high Wnt activity in CSCs but can also instruct more differentiated tumour cells to activate the Wnt pathway and thereby restore clonogenicity or tumorigenicity (summarized in Fig. 8). We have excluded the possibility that this is due to the activation of a small subset of residual CSCs in the TOP–GFP^{low} population: the effect is too rapid and occurs well before any cell expansion has taken place. However, to what extent these cells possess unlimited replicative potential, which is a crucial hallmark in the definition of a CSC, remains to be elucidated by repetitive isolations and subsequent injections.

Nonetheless, the potential of these cells to proliferate extensively and form tumours that contain a similar Wnt signalling heterogeneity to that observed with TOP–GFP^{high}-induced tumours warrants the conclusion that the microenvironment is central to the growth of colon cancers under these conditions. Previous observations by us and others have suggested that brain CSCs are also supported by (perivascular) endothelial cells[33,34]. Although those studies did not reveal whether differentiated tumour cells can regain stemness, they may point to a similar relation between CSCs and microenvironment and suggest that the CSC phenotype may be a much more dynamic characteristic than has previously been assumed.

In this light we note that there is an ongoing debate in the field on the existence and incidence of CSCs within different tumours. This has in part been explained by immune responses observed in xenotransplantation assays[35–37] and by differences between tumours. Our present observations indicate that the usage of fully immune-deficient mice does not annihilate the difference between TOP–GFP^{high} and TOP–GFP^{low} cells, proving that cancer stemness is not due to a different sensitivity to immune control. However, we feel that our data, by implicating the microenvironment as a dominant factor in CSC, can potentially shed new light on this controversy. One could envisage that tumours such as late-stage melanoma have become independent of the signals elicited by the microenvironment and therefore do not show a clear-cut CSC organization[37]. Alternatively, a subset of tumours could be more effective in modulating the microenvironment or could simply be more receptive to the local environment at the site of injection. In this light we note that our observations indicate a rapid attraction or formation of myofibroblasts at the site of tumour formation. Combined with the observation that differentiated tumour cells induce tumours when co-injected with such myofibroblasts, this suggests that differentiated tumour cells simply fail to create the right environment and therefore fail to show tumour-initiating capacity. This conclusion would have far-reaching consequences when discussing tumour therapy. As CSC have been shown to be relatively resistant to therapy[14,38–40], present strategies are aimed at developing CSC selective therapies, thereby attacking the tumour at its root. However, this approach would be frustrated by plasticity of the system, which would simply lead to CSC regeneration from the differentiated tumour compartment. In contrast, the model we propose indicates that attention should be directed to the potential opportunity offered by the interface of the microenvironment and the CSC as a therapeutic target.

It has previously been shown that nuclear β-catenin localization was predominantly observed in the invasive regions of colon carcinomas, that is, at the leading edges[10]. These observations concur with our hypothesis

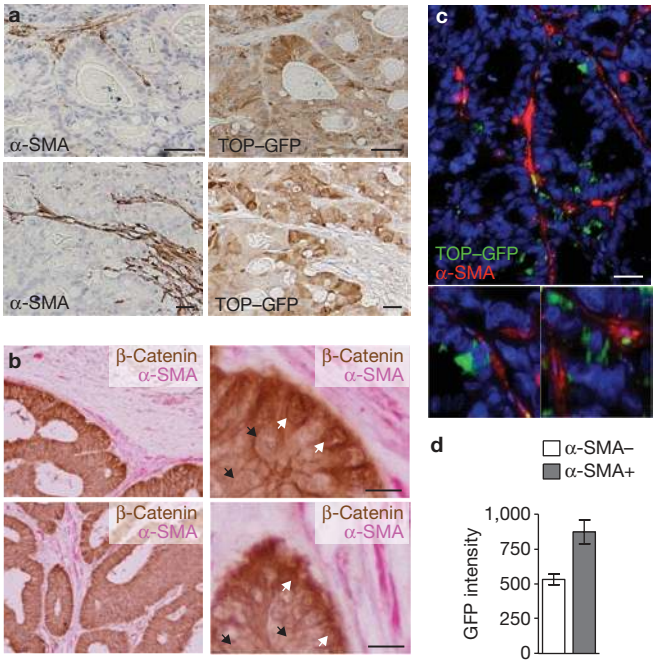

e

			Cells Injected			
Line	Fraction	Condition	10	100	1,000	5,000
C100.B5	TOP–GFP^{low}	–	0/6	0/6	1/6	3/6
	TOP–GFP^{high}	–	3/6	5/6	6/6	–
	TOP–GFP^{low}	+ MFCM	0/6	4/6	5/6	6/6
C100.G7	TOP–GFP^{low}	–	0/6	0/6	0/6	0/6
	TOP–GFP^{intermediate}	–	0/6	0/6	2/6	–
	TOP–GFP^{high}	–	0/6	2/6	3/6	–
	TOP–GFP^{low}	+ MFCM	0/6	1/6	4/6	4/6
	TOP–GFP^{low}	+ MF	0/6	0/6	3/6	6/6

Figure 7 Myofibroblasts restore tumorigenicity in TOP–GFP^{low} Wnt-active cells and co-localize with highly Wnt-active cells *in vivo*. (**a**) Myofibroblasts are present in the stroma of TOP–GFP xenografts as demonstrated by α-SMA-positive cells and localize close to cells expressing TOP–GFP as detected by α-GFP immunohistochemistry in consecutive slides. Scale bars, 50 μm. (**b**) In human colorectal cancer specimens, cells positive for nuclear β-catenin (brown) show an intimate relationship with α-SMA-positive myofibroblasts (purple). The right panels show enlargements; white and black arrowheads indicate tumour cells with and without nuclear β-catenin, respectively. (**c**) Immunofluorescence co-staining for α-SMA and GFP indicates a close relationship between TOP–GFP^{high} cells and myofibroblasts. Scale bar, 50 μm. (**d**) Quantification of TOP–GFP intensity in areas of epithelial cells that are next to α-SMA cells reveals a relationship between myofibroblasts and enhanced Wnt signalling (Student's *t*-test, $P < 0.001$; see Methods for details). (**e**) *In vivo* transfer of TOP–GFP-transduced cultures. Cell numbers from the indicated populations were injected into nude mice after FACS. The number of successful tumour initiations after nine weeks out of six injections for each condition is shown. Injection of TOP–GFP^{low} cells with myofibroblasts (MF) or after treatment with MFCM shows enhanced tumour growth in comparison with TOP–GFP^{low} cells alone. The upper part of the table is a partial representation of Fig. 3a.

that myofibroblasts, which are present at high density at the tumour front, could direct Wnt activation. This suggests a framework in which stromal components, in this case HGF-producing myofibroblasts, stimulate CSC features of cancer cell populations mainly at the tumour edges and simultaneously promote the invasion and spread of the malignancy into the surrounding tissue, as has also been suggested previously[41]. The fact

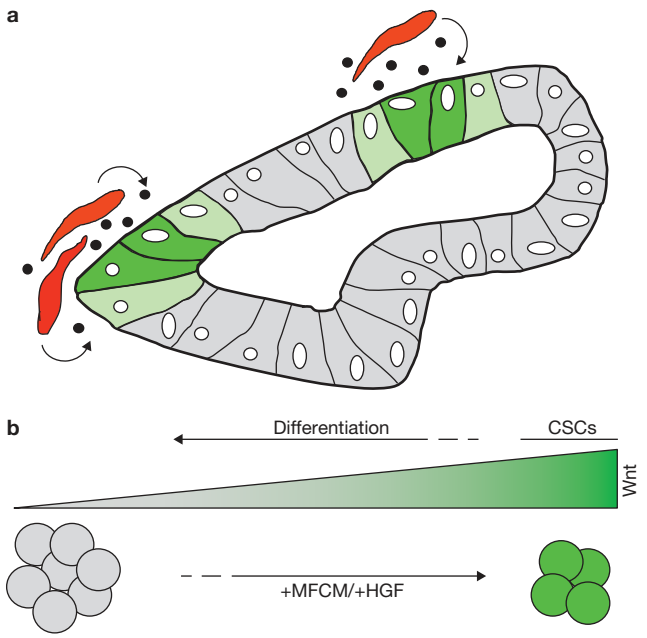

Figure 8 Schematic representation of the proposed model. (**a**) Cells with a high Wnt signal activity (depicted in green) reside close to stromal myofibroblasts (red) in colorectal cancer tissue. Cells with a relatively low Wnt activity are depicted in grey. Tumour-associated myofibroblasts secrete factors such as HGF (black dots) that stimulate Wnt signalling. (**b**) Stimulation of the Wnt signalling cascade in differentiated colon cancer cells, characterized by low Wnt signalling activity, restores CSC characteristics. These include expression of CSC markers and tumorigenicity. Taken together, these results suggest a pivotal role for the environment in determining CSC features of colon cancer cells.

that HGF/c-Met overexpression is correlated with colon cancer progression only strengthens this notion[30,42]. This is not merely due to enhanced scattering of tumour cells by HGF, because c-Met silencing also induces almost complete regression of already established metastases in an experimental model[43]. This indicates a constitutive need for c-Met-mediated signals in the growth or maintenance of metastases and is consistent with a role for HGF in CSC maintenance.

The tight relationship between CSC properties, invasion and microenvironment is corroborated by findings that suggest that the CSC phenotype, epithelial–mesenchymal transition (EMT), invasion and microenvironmental interactions are closely associated in breast cancer[44]. In addition, plasticity takes a central position here because activation of the EMT-promoting factors Snail or Twist generates CSCs from more differentiated tumour cells, which revert when these EMT-promoting signals are not maintained[44]. Intriguingly, the original studies on MDCK cell scattering, which spurred the interest in EMT[45], in essence showed that HGF was a potent EMT inducer that was in later work related to the induction of Snail in epithelial cancer cells[46]. Moreover, in normal development Wnt signals are crucially tethered to the induction of EMT[47]. Taken together, these observations therefore point to the hypothesis that colon cancer stemness is partly defined by environmental cues, such as HGF, and can be induced in more differentiated tumour cells by the microenvironment and may therefore be closely related to EMT. This has important consequences for the way in which we perceive CSCs as critical therapeutic targets, shifting the attention from the CSC to its environment. □

METHODS

Methods and any associated references are available in the online version of the paper at http://www.nature.com/naturecellbiology/

Note: Supplementary Information is available on the Nature Cell Biology website.

ACKNOWLEDGEMENTS

The authors are indebted to the work performed by Willem Bemelman and Thomas van Gulik, surgeons at the AMC without whom the studies described here would not have been possible. In addition, we thank Riccardo Fodde for constructive discussions on CSCs and Wnt, and the animal care takers for their work for this project. Finally, we thank Berend Hooibrink and Toni van Capel for assistance with fluorescence-activated cell sorting experiments. This work was supported by a VICI grant from the Netherlands Organisation for Scientific Research and a Dutch Cancer Society (KWF Kankerbestrijding) grant (2009-4416) (to J.P.M.), an Academisch Medisch Centrum (AMC) fellowship (to L.V. and F.d.S.M.), the AMC Graduate School (to K.K.) and by the Associazione Italiana per la Ricerca sul Cancro (AIRC) (to G.S. and M.T.).

AUTHOR CONTRIBUTIONS

L.V., F.d.S.M., M.v.d.H., K.C., J.H.d.J., T.B., J.B.T., H.R., M.R.S., K.K. designed and conducted experiments. M.T. and C.M. isolated and cultured CSC lines, D.J.R., G.S. and J.P.M. planned and supervised the experiments. L.V., F.d.S.M and J.P.M wrote the manuscript.

COMPETING FINANCIAL INTERESTS

The authors declare no competing financial interests.

Published online at http://www.nature.com/naturecellbiology
Reprints and permissions information is available online at http://npg.nature.com/reprintsandpermissions/

1. Fearon, E. R. & Vogelstein, B. A genetic model for colorectal tumorigenesis. *Cell* **61,** 759–767 (1990).
2. Clevers, H. Wnt/β-catenin signaling in development and disease. *Cell* **127,** 469–480 (2006).
3. Bienz, M. & Clevers, H. Linking colorectal cancer to Wnt signaling. *Cell* **103,** 311–320 (2000).
4. Vogelstein, B. *et al.* Genetic alterations during colorectal-tumor development. *N. Engl. J. Med.* **319,** 525–532 (1988).
5. Tetsu, O. & McCormick, F. β-Catenin regulates expression of cyclin D1 in colon carcinoma cells. *Nature* **398,** 422–426 (1999).
6. He, T. C. *et al.* Identification of c-*MYC* as a target of the APC pathway. *Science* **281,** 1509–1512 (1998).
7. Korinek, V. *et al.* Depletion of epithelial stem-cell compartments in the small intestine of mice lacking Tcf-4. *Nature Genet.* **19,** 379–383 (1998).
8. Groden, J. *et al.* Response of colon cancer cell lines to the introduction of APC, a colon-specific tumor suppressor gene. *Cancer Res.* **55,** 1531–1539 (1995).
9. van de Wetering, M. *et al.* The β-catenin/TCF-4 complex imposes a crypt progenitor phenotype on colorectal cancer cells. *Cell* **111,** 241–250 (2002).
10. Brabletz, T. *et al.* Variable β-catenin expression in colorectal cancers indicates tumor progression driven by the tumor environment. *Proc. Natl Acad. Sci. USA* **98,** 10356–10361 (2001).
11. Fodde, R. & Brabletz, T. Wnt/β-catenin signaling in cancer stemness and malignant behavior. *Curr. Opin. Cell Biol.* **19,** 150–158 (2007).
12. Vermeulen, L., Sprick, M. R., Kemper, K., Stassi, G. & Medema, J. P. Cancer stem cells—old concepts, new insights. *Cell Death. Differ.* **15,** 947–958 (2008).
13. O'Brien, C. A., Pollett, A., Gallinger, S. & Dick, J. E. A human colon cancer cell capable of initiating tumour growth in immunodeficient mice. *Nature* **445,** 106–110 (2007).
14. Todaro, M. *et al.* Colon cancer stem cells dictate tumor growth and resist cell death by production of interleukin-4. *Cell Stem Cell* **1,** 389–402 (2007).
15. Dalerba, P. *et al.* Phenotypic characterization of human colorectal cancer stem cells. *Proc. Natl Acad. Sci. USA* **104,** 10158–10163 (2007).
16. Ricci-Vitiani, L. *et al.* Identification and expansion of human colon-cancer-initiating cells. *Nature* **445,** 111–115 (2007).
17. Vermeulen, L. *et al.* Single-cell cloning of colon cancer stem cells reveals a multilineage differentiation capacity. *Proc. Natl Acad. Sci. USA* **105,** 13427–13432 (2008).
18. Reya, T. *et al.* A role for Wnt signalling in self-renewal of haematopoietic stem cells. *Nature* **423,** 409–414 (2003).
19. Barker, N. *et al.* Identification of stem cells in small intestine and colon by marker gene *Lgr5*. *Nature* **449,** 1003–1007 (2007).
20. van der Flier, L. G. *et al.* Transcription factor achaete scute-like 2 controls intestinal stem cell fate. *Cell* **136,** 903–912 (2009).
21. Yeung, T. M., Gandhi, S. C., Wilding, J. L., Muschel, R. & Bodmer, W. F. Cancer stem cells from colorectal cancer-derived cell lines. *Proc. Natl Acad. Sci. USA* **107,** 3722–3727 (2010).
22. Kai, K. *et al.* Maintenance of HCT116 colon cancer cell line conforms to a stochastic model but not a cancer stem cell model. *Cancer Sci.* **100,** 2275–2282 (2009).

23. Clarke, M. F. *et al.* Cancer stem cells—perspectives on current status and future directions: AACR Workshop on cancer stem cells. *Cancer Res.* **66,** 9339–9344 (2006).
24. Karnoub, A. E. *et al.* Mesenchymal stem cells within tumour stroma promote breast cancer metastasis. *Nature* **449,** 557–563 (2007).
25. Sato, T. *et al.* Single Lgr5 stem cells build crypt–villus structures *in vitro* without a mesenchymal niche. *Nature* **459,** 262–265 (2009).
26. Yen, T. H. & Wright, N. A. The gastrointestinal tract stem cell niche. *Stem Cell Rev.* **2,** 203–212 (2006).
27. Boon, E. M., van der, N. R., van de, W. M., Clevers, H. & Pals, S. T. Wnt signaling regulates expression of the receptor tyrosine kinase met in colorectal cancer. *Cancer Res.* **62,** 5126–5128 (2002).
28. Rasola, A. *et al.* A positive feedback loop between hepatocyte growth factor receptor and beta-catenin sustains colorectal cancer cell invasive growth. *Oncogene* **26,** 1078–1087 (2007).
29. Brembeck, F. H. *et al.* Essential role of BCL9-2 in the switch between β-catenin's adhesive and transcriptional functions. *Genes Dev.* **18,** 2225–2230 (2004).
30. Di Renzo, M. F. *et al.* Overexpression and amplification of the Met/HGF receptor gene during the progression of colorectal cancer. *Clin. Cancer Res.* **1,** 147–154 (1995).
31. Ng, S. S. *et al.* Phosphatidylinositol 3-kinase signaling does not activate the Wnt cascade. *J. Biol. Chem.* **284,** 35308–35313 (2009).
32. Fang, D. *et al.* Phosphorylation of β-catenin by AKT promotes β-catenin transcriptional activity. *J. Biol. Chem.* **282,** 11221–11229 (2007).
33. Borovski, T. *et al.* Tumor microvasculature supports proliferation and expansion of glioma-propagating cells. *Int. J. Cancer* **125,** 1222–1230 (2009).
34. Calabrese, C. *et al.* A perivascular niche for brain tumor stem cells. *Cancer Cell* **11,** 69–82 (2007).
35. Shackleton, M., Quintana, E., Fearon, E. R. & Morrison, S. J. Heterogeneity in cancer: cancer stem cells versus clonal evolution. *Cell* **138,** 822–829 (2009).
36. Kelly, P. N., Dakic, A., Adams, J. M., Nutt, S. L. & Strasser, A. Tumor growth need not be driven by rare cancer stem cells. *Science* **317,** 337 (2007).
37. Quintana, E. *et al.* Efficient tumour formation by single human melanoma cells. *Nature* **456,** 593–598 (2008).
38. Guan, Y., Gerhard, B. & Hogge, D. E. Detection, isolation, and stimulation of quiescent primitive leukemic progenitor cells from patients with acute myeloid leukemia (AML). *Blood* **101,** 3142–3149 (2003).
39. Guzman, M. L. *et al.* Preferential induction of apoptosis for primary human leukemic stem cells. *Proc. Natl Acad. Sci. USA* **99,** 16220–16225 (2002).
40. Bao, S. *et al.* Glioma stem cells promote radioresistance by preferential activation of the DNA damage response. *Nature* **444,** 756–760 (2006).
41. Brabletz, T., Jung, A., Spaderna, S., Hlubek, F. & Kirchner, T. Opinion: migrating cancer stem cells—an integrated concept of malignant tumour progression. *Nature Rev. Cancer* **5,** 744–749 (2005).
42. Kammula, U. S. *et al.* Molecular co-expression of the c-Met oncogene and hepatocyte growth factor in primary colon cancer predicts tumor stage and clinical outcome. *Cancer Lett.* **248,** 219–228 (2007).
43. Corso, S. *et al.* Silencing the MET oncogene leads to regression of experimental tumors and metastases. *Oncogene* **27,** 684–693 (2008).
44. Mani, S. A. *et al.* The epithelial–mesenchymal transition generates cells with properties of stem cells. *Cell* **133,** 704–715 (2008).
45. Stoker, M. & Perryman, M. An epithelial scatter factor released by embryo fibroblasts. *J. Cell Sci.* **77,** 209–223 (1985).
46. Grotegut, S., von, S. D., Christofori, G. & Lehembre, F. Hepatocyte growth factor induces cell scattering through MAPK/Egr-1-mediated upregulation of Snail. *EMBO J.* **25,** 3534–3545 (2006).
47. Moustakas, A. & Heldin, C. H. Signaling networks guiding epithelial–mesenchymal transitions during embryogenesis and cancer progression. *Cancer Sci.* **98,** 1512–1520 (2007).

METHODS

Cell culture. CSCs were isolated from different patients in accordance with the rules of the medical ethical committee of the AMC and University of Palermo and Heidelberg, and named after their site of origin. Primary samples were named Co and liver metastases were named LM, both followed by a number representing the isolation. CSCs were cultured in modified neurobasal A medium containing N2 supplement (Invitrogen), Lipid Mixture-1 (Sigma), basic fibroblast growth factor (bFGF; 20 ng ml^{-1}) and epidermal growth factor (EGF; 50 ng ml^{-1}). Colon cancer cell lines were cultured in Iscove's modified defined medium (IMDM) plus 10% FCS, glutamine and penicillin/streptomycin. 18Co cells were purchased from the American Type Culture Collection and maintained in DMEM medium supplemented with 10% FCS and 1% glutamine.

Colon CSC cultures were derived as described previously[14]. In brief, primary resected human colon carcinomas were digested enzymatically for 1 h with a mixture of collagenase (1.5 mg ml^{-1}; Roche) and hyaluronidase (20 μg ml^{-1}) at 37 °C and shaken repeatedly. The dissociated sample was then filtered (40 μm pore size) and washed in CSC medium. Erythrocytes and cell debris were removed by Lympholyte (M; Cedarlane) centrifugation. Cells were then washed with CSC medium and subsequently cultured. For isolation of primary myofibroblasts, colorectal specimens were first cut into small pieces and incubated for 30 min with 1 mM EDTA (Sigma) at 37 °C with repetitive shaking to remove epithelial cells. Samples were washed with Hanks balanced salt solution between each incubation and then digested enzymatically for 30 min with collagenase (1.5 mg ml^{-1}; Roche) at 37 °C with shaking. Cells were then washed and plated at high density with DMEM supplemented with 10% FCS and 1% non-essential amino acids.

Lentiviral and luciferase reporter assays. TCF/LEF reporter driving expression of GFP (TOP–GFP) was a gift from Laurie Ailles and was described previously[18]. Spheroidal cultures were transduced lentivirally with either the TOP–GFP or constitutive CMV–GFP or PGK–GFP constructs. Generation of single-cell-derived cultures was performed by FACSaria (BD Biosciences) single-cell plating in 96-well ultralow-adhesion plates (Corning) containing stem-cell medium. We stringently gated on single, propidium iodide-negative/GFP-positive cells. After visible spheres arose, they were transferred to ultralow-adhesion flasks (Corning) and expanded. Luciferase assays were performed as recommended by the manufacturer (SA Biosciences). Cells were transiently transfected (FuGENE 6; Roche) with a mixture of inducible TCF/LEF-responsive firefly luciferase and constitutively expressed *Renilla* luciferase (40:1), or with a negative control containing a mixture of non-inducible firefly luciferase and constitutively expressed *Renilla* luciferase (40:1). All experiments were performed in triplicate. Cells were lysed in luciferase reporter lysis buffer and monitored for luciferase and *Renilla* activity with a Dual-Luciferase Reporter Assay System (Promega). Cells were starved for 12 h and stimulated for 12–16 h with indicated factors.

Limiting-dilution assay. Cells from different GFP intensities were deposited at 1, 2, 4, 6, 8, 12, 16, 20 and 24 cells per well. Clonal frequency and statistical significance were evaluated with the Extreme Limiting Dilution Analysis (ELDA) 'limdil' function (http://bioinf.wehi.edu.au/software/elda/index.html).

Immunohistochemistry and western blot antibodies and reagents. Immunofluorescence and/or immunohistochemistry were performed on paraffin-embedded sections or on cytospins as described[17]. The following antibodies were used for immunohistochemistry and immunofluorescence: anti-β-catenin (Cell Signaling Technology, 1:100 dilution; Transduction Labs, 1:250), anti-GFP (Roche, 1:500), anti-α-SMA (Abcam, 1:100), anti-Vimentin (Abcam, 1:100), anti-desmin (Neomarkers, 1:100), anti-HGF (R&D Systems, 1:100), anti-cytokeratin 20 (Genetex, 1:250), anti-FAPB2 (Abcam, 1:200) and anti-Muc2 (Abcam, 1:200). The following antibodies were used for western blotting: anti-β-actin (Sigma, 1:1,000), anti-phospho-Met (Tyr 1234/1235, 1:500), anti-Met (25H2, 1:500), anti-phospho-Akt (Ser 473, 1:500), anti-Akt (1:500), anti-phospho-Gsk3(Ser 9, 1:500), anti-Gsk3 (1:1,000), anti-phospho-β-catenin (Thr 41/Ser 45, 1:500; Ser 552, 1:500) and anti-β-catenin (1:1,000); all except the anti-β-actin were purchased from Cell Signaling Technology. Alcian Blue staining was performed with Alcian Blue 8GX (Sigma). Haematoxylin/eosin staining was performed with Ehrlich haematoxylin/eosin solution (Sigma). Western blotting was performed as described[48]. Full blots are shown in Supplementary Information, Fig. S7.

Conditioned medium, enzyme-linked immunosorbent assay (ELISA) and cytokine array, cytokines and inhibitors. A total of 7.5×10^5 18Co cells were seeded in 75-cm^2 flasks. On the next day, cells were washed twice with PBS and incubated for 24 h with 10 ml of CSC medium without EGF and bFGF. MFCM was then collected and cleared by centrifugation and used at 1:2 dilution.

A cytokine/chemokine array kit (Ray Biotech Inc.) was used to detect a panel of 79 secreted cytokines and chemokines in MFCM. The manufacturer's recommended protocol was used. Human recombinant HGF (50 ng ml^{-1}) was from Relia Tech. Inc. A novel small molecule inhibiting c-Met phosphorylation (PHA665752) was provided by Pfizer. A neutralizing HGF antibody (R&D Systems) was used to deplete HGF from the MFCM. In brief, MFCM was incubated for 1 h at 37 °C with the neutralizing antibody (10 μg ml^{-1}) before use in the stimulation assay. HGF secretion was quantified by quantitative ELISA according to manufacturer's instructions (R&D).

Flow cytometry. Flow cytometry was performed on trypsin-dissociated TOP–GFP CSC cultures with AC133 (Miltenyi Biotec, 1:100), CD44 (BD Biosciences, 1:100), CD166 (R&D Systems, clone 105901, 1:100), CD24 (BD Biosciences, 1:100), CD29 (BD Biosciences, 1:100) and c-Met (Upstate, 1:100). Dead cells were excluded with propidium iodide.

RNA extraction, microarray and PCR. Total RNA from cells comprising the lowest and highest 10% TOP–GFP of spheroidal SCD cultures was extracted with Trizol reagent (Invitrogen) in accordance with the manufacturer's protocol. RNA concentration was determined with NanoDrop ND-1000, and quality was determined using the RNA 6000 Nano assay on the Agilent 2100 Bioanalyzer (Agilent Technologies). Affymetrix microarray analysis, fragmentation of RNA, labelling, hybridization to Human Genome U133 Plus 2.0 microarrays, and scanning were performed in accordance with the manufacturer's protocol (Affymetrix). Microarray data can be viewed online (http://www.ncbi.nlm.nih.gov/geo/index.html) under GEO accession number GSE17375. Real time RT–PCR was performed with SYBR green (Abgene) in accordance with the manufacturer's instructions on a Bio-Rad MyiQ Thermal cycler. For primers used see Supplementary Information, Table S2.

***In vivo* tumour propagation.** Mice experiments were performed in accordance with the ethical committee of the AMC. For transplantation of cancer cells, 30 spheres (about 100 cells per sphere) suspended in 100 μl of PBS/BSA admixed with Matrigel at a 1:1 ratio were injected subcutaneously into nude mice (Hsd:Athymic Nude/Nude) (Harlan). After 3–8 weeks visible tumours arose. When the tumour size reached 1 cm^3, mice were killed and tumours were processed either for analysis or for culture *in vitro*. For *in vivo* limiting-dilution injection, TOP–GFP-transduced cultures or established xenografts from the TOP–GFP cultures were dissociated and 1, 10, 100, 1,000 and 5,000 cells from the 10% lowest, 10% highest or total TOP–GFP intensities were deposited, by FACS, in a 96-well plate containing CSC medium, admixed with Matrigel, and injected as described above. For myofibroblast co-injection experiments 50,000 18Co cells were plated in 96-well plates; TOP–GFP^{low} cells were added by FACS deposition in the indicated amounts and injected as described. For MFCM stimulation of TOP–GFP^{low} cells, cells were deposited by FACS in MFCM and incubated at 37 °C for 2 h; afterwards cells and MFCM were admixed 1:1 with Matrigel and injected. For single-cell injection single cells were deposited from the 0.5% highest TOP–GFP cells, and single-cell deposition was confirmed microscopically.

Co-immunostaining and quantification. Paraffin-embedded xenografts from TOP–GFP cultures were co-stained with anti-GFP and anti-α-SMA antibody. GFP intensities of epithelial cell regions in the direct presence or not of α-SMA-positive cells were quantified with an inverted fluorescence microscope (Zeiss), using the Axiovision software. Serial sections ($n = 45$) and multiple fields per section were scored. Student's *t*-test was used for statistical significance. Paraffin-embedded primary human specimens were co-stained with α-SMA (Abcam) and anti-β-catenin (Transduction Labs) and then incubated with anti-rabbit-AP/anti-mouse-HRP (Powervison) (1:1). RED Alkaline Phosphatase substrate (Vector) followed by DAB+ (Dako) were applied to the slides.

48. Tuynman, J. B. *et al.* Cyclooxygenase-2 inhibition inhibits c-Met kinase activity and Wnt activity in colon cancer. *Cancer Res.* **68,** 1213–1220 (2008).

nature cell biology

DOI: 10.1038/ncb2048

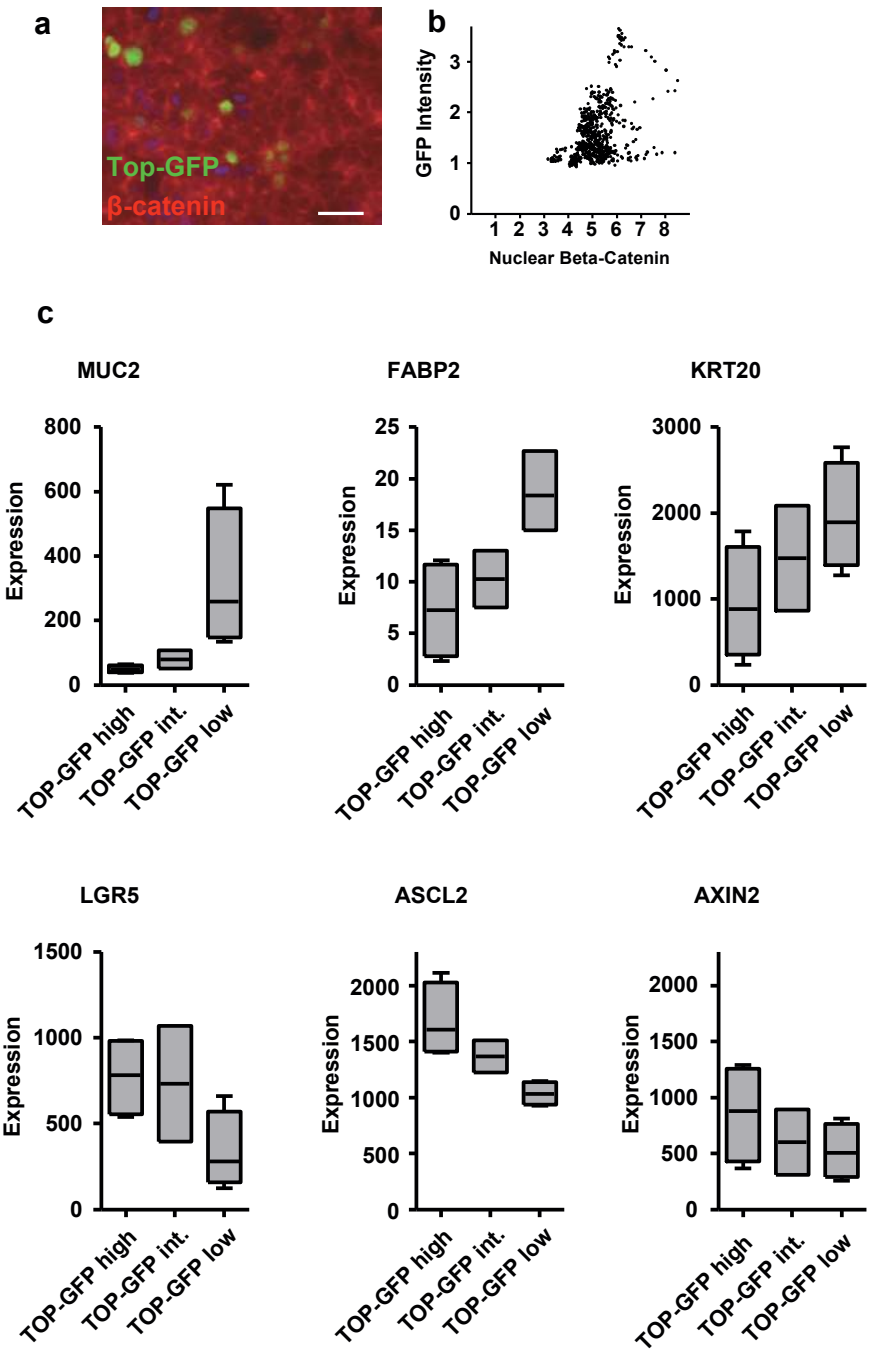

Figure S1 TOP-GFP expression and relation with nuclear β-catenin, wnt targets and differentiation markers. (**a**) Co-immunostaining of TOP-GFP spheroid culture with GFP and β-catenin antibody demonstrates a clear correlation between TOP-GFP levels and nuclear localization of β-catenin (scale bar, 50μm), quantification shown in (**b**). (**c**) Microarray analysis of a specific gene-set in high, intermediate and low TOP-GFP cell fractions indicates gradual increase in differentiation marker expression and a decrease in Wnt target gene expression from TOP-GFP^{high} to TOP-GFP^{low} populations (Each box plot represents a minimal of two data points from separate single-cell cloned TOP-GFP CSC cultures). Genes were picked based on significant differences observed in Fig 1d.

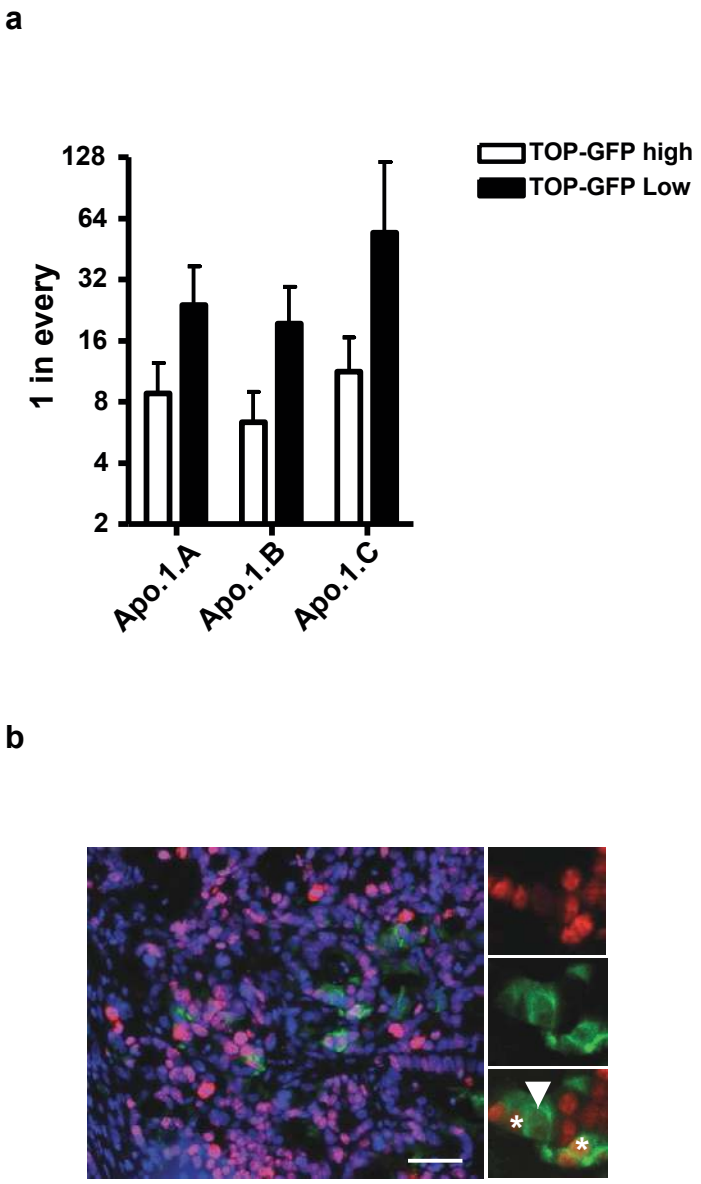

Figure S2 Limiting dilution on various clones, Ki-67 staining. (**a**) Limiting dilution assay and clonogenic potential of 3 independent lines derived from the same patient as Apo.1 (Apo.1.A, Apo.1.B and Apo.1.C). Errors bars represent 95% CI. Representative examples are shown. See Methods for details on limiting dilution assays. (**b**) Ki-67 co-staining with GFP in TOP-GFP xenografts. Ki-67 positivity encompasses both GFP positive and negative cells. Scale bar, 100μm.

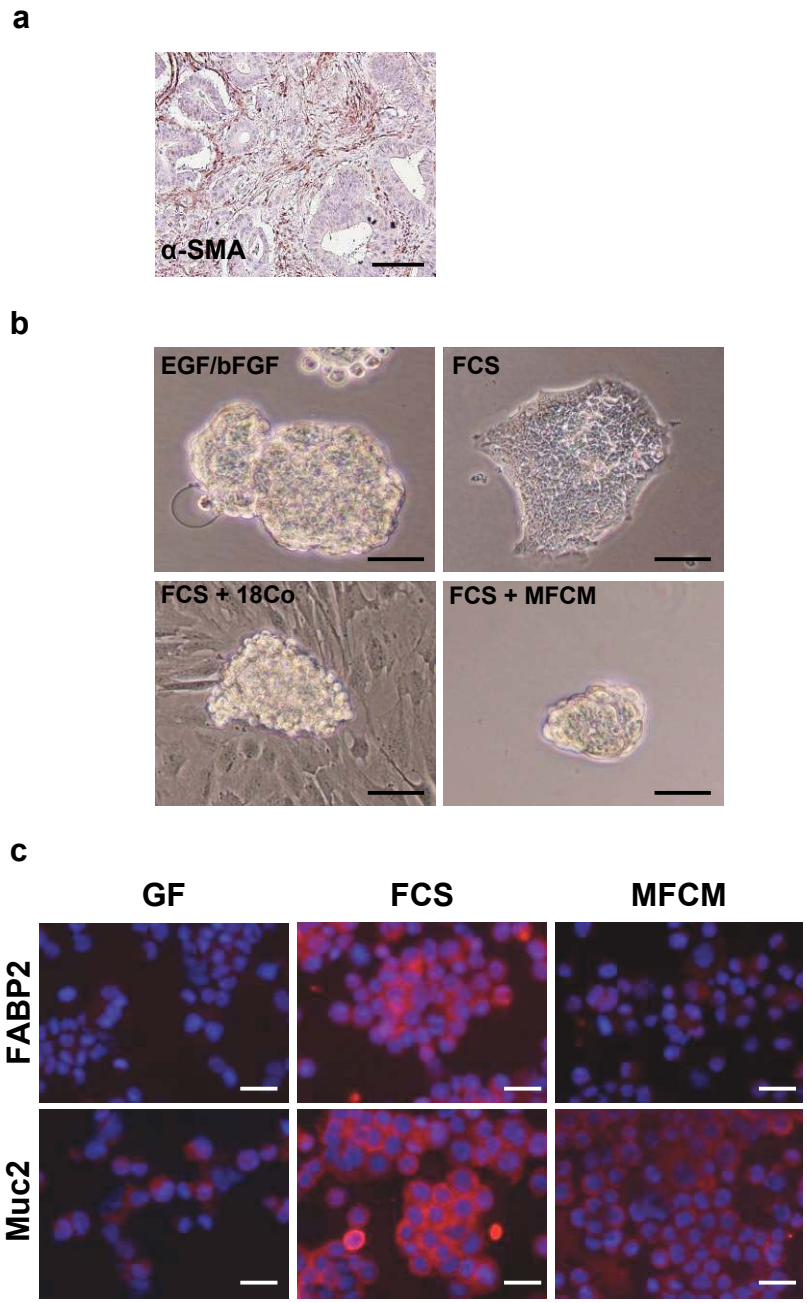

Figure S3 Myofibroblasts prevent differentiation of colon CSCs. (**a**) Immunohistochemistry for α-SMA shows myofibroblasts in the stroma of primary human colorectal malignancies. (Scale bar, 50μm) (**b**) Phase contrast pictures to show morphological differentiation of CSC. Upper left represents a spheroid culture growing in medium containing EGF and bFGF, upper right is after differentiation in 2% FCS. Lower left is differentiation with 2% FCS, but plated on myofibroblasts (18Co) and lower right is differentiation with FCS in the presence of MFCM. (Scale bar, 20μm) (**c**) Immunofluorescence for FABP2 and Muc2 on cytospins of spheroid cells (EGF/bFGF) or cells induced to differentiate with 2% FCS in the absence (middle) or presence of MFCM (right). (Scale bar, 20μm)

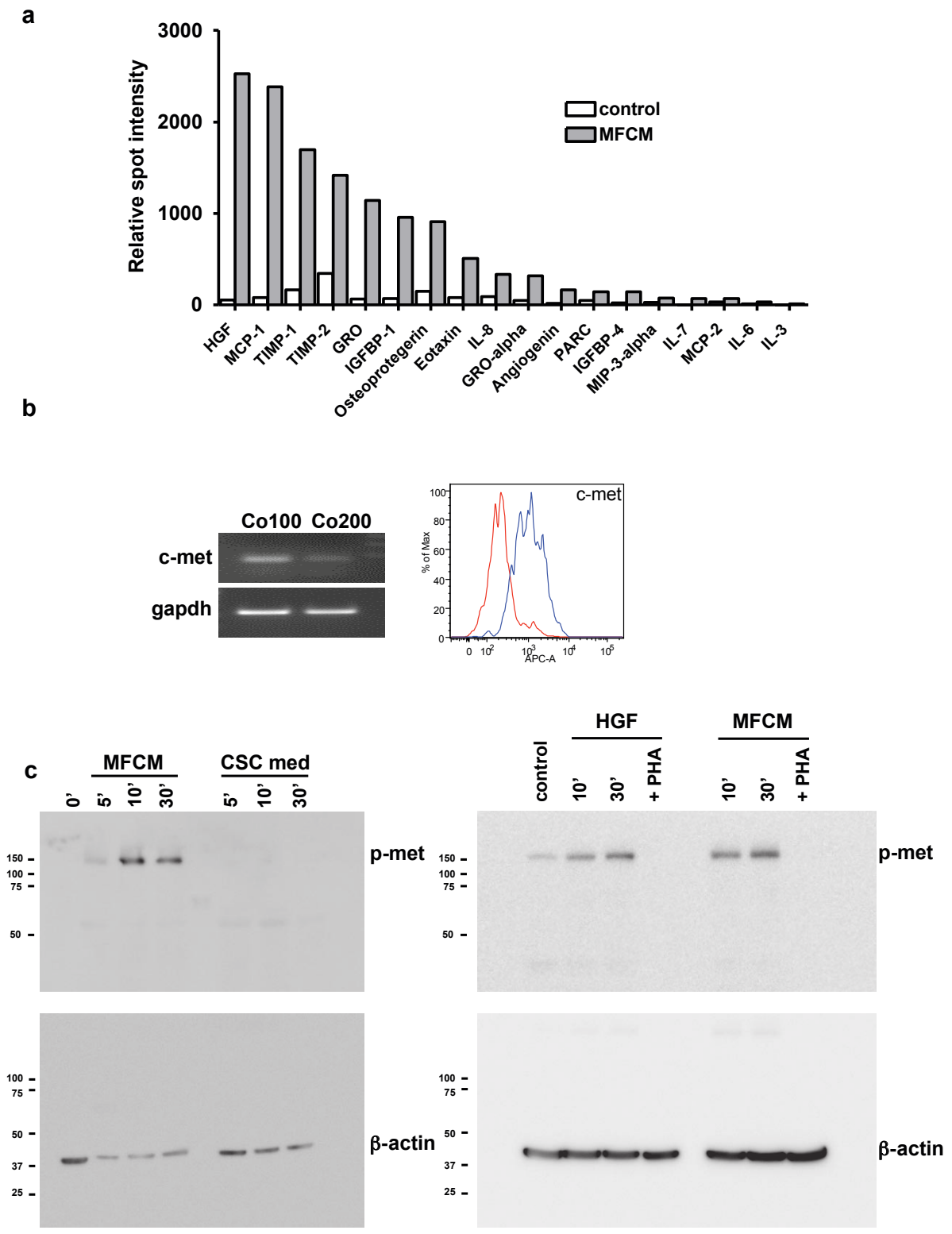

Figure S4 Myofibroblasts produce HGF and human colon CSCs express c-Met. (**a**) A graph depicting the detected secreted factors in MFCM (see Methods for details). (**b**) PCR showing expression of c-Met in spheroid cultured colon CSCs. Right panel shows FACS analysis for c-Met. (red; background and blue; c-Met) (**c**) Full blot of phospho-c-Met and β-actin of Co200 stimulated with 18Co conditioned medium (MFCM) or CSC control medium for the time indicated.

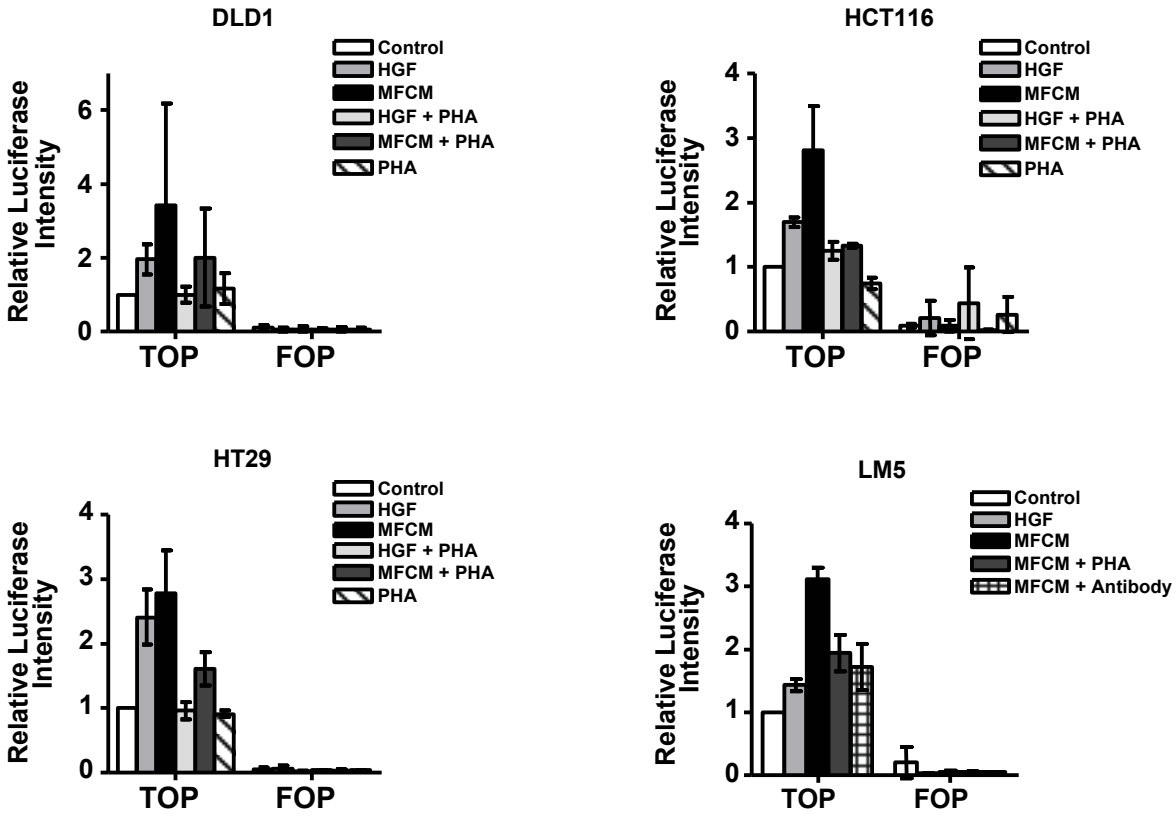

Figure S5 TOP/FOP assay on various lines and with various conditions. Depicted are the results of TOP/FOP assays on different human colon cancer lines including several established colorectal cancer lines (DLD1, HCT116, HT29). LM5 is a liver metastasis derived primary CSC line. The stimulatory effect of MFCM is HGF dependent. Error bars represent SEM (n=3), data from at least 2 replicates is shown.

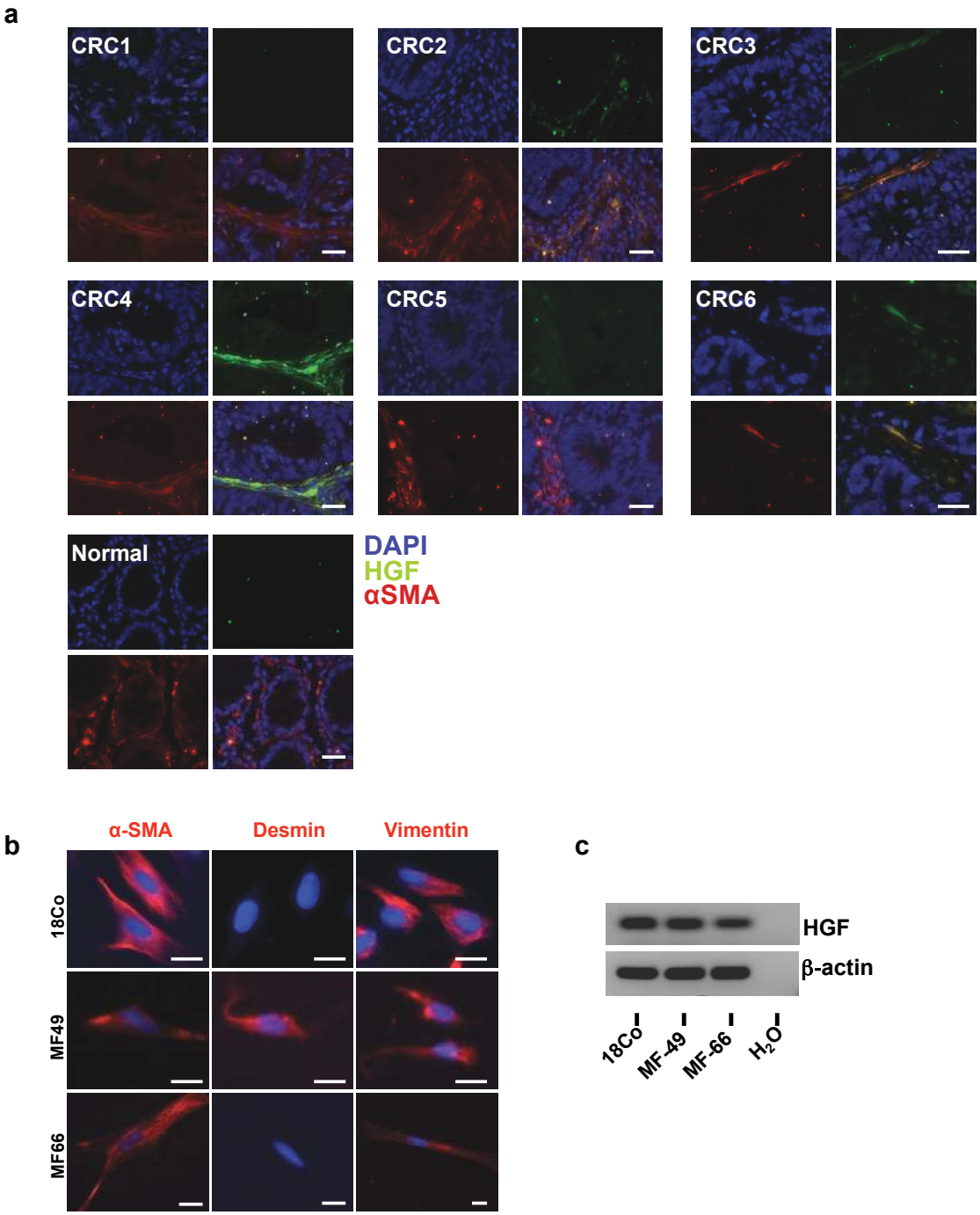

Figure S6 Human colon carcinoma associated myofibroblasts express HGF. Six different human primary colorectal cancer specimens and one normal human colon specimen was stained for both HGF and α-SMA. In 4 out of 6 samples we detected HGF in α-SMA-positive cells. Scale Bars, 50μm. (**b**) Both an established colon myofibroblast line (18Co) as well as two primary lines (MF49, MF66) isolated from colorectal cancer patients express markers associated with myofibroblasts (Scale bars, 20μm) and reveal HGF production by (**c**) PCR.

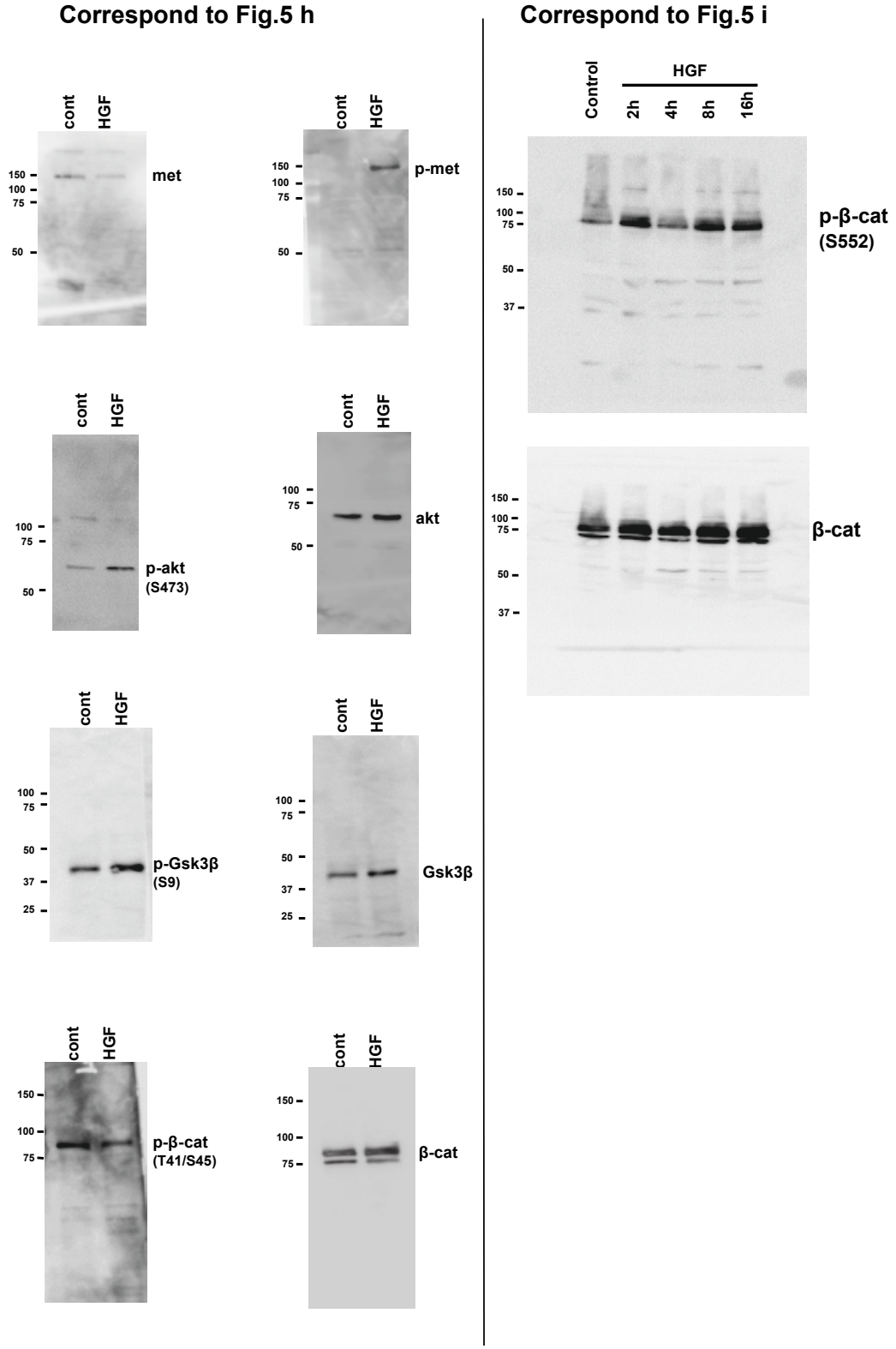

Figure S7 Full blots. Represented are the full Western blots of Fig. 5h and i.

Table S1 Genes showing most differential expression between TOP-GFP^{high} and TOP-GFP^{low} cell populations. A list of the most differentially regulated genes in the TOP-GFP^{high} versus TOP-GFP^{low} fractions from two different single cell cultures is summarized in Table S1, indicated values represent Log_2 fold-changes.

Table S2 List of primers used in this study.

Table S1

Gene	Probeset	G7	A4
FABP1	*205892_s_at*	-4.9	-1.7
AKR1B10	*206561_s_at*	-4.6	-2.5
MUC2	*204673_at*	-3.6	-1.8
ST6GALNAC1	*227725_at*	-3.2	-1.5
GCNT3	*219508_at*	-2.7	-1.3
SPINK4	*207214_at*	-2.4	-1.5
HEPACAM2	*242601_at*	-1.9	-1.7
GMPR	*204187_at*	1.8	1.5
CAB39L	*225915_at*	2.3	1.4
TSPAN5	*209890_at*	2.5	1.5
NEURL1B	*225355_at*	2.7	1.3
TUBB2B	*214023_x_at*	2.8	1.6
LGR5	*213880_at*	2.9	1.3
SERPINI1	*205352_at*	3.0	1.9
LEF1	*221558_s_at*	3.0	1.6
LRP4	*212850_s_at*	3.1	1.4
CXCR4	*217028_at*	3.3	2.7
SP5	*235845_at*	3.7	1.9
DEFA5	*207529_at*	5.1	3.9
APCDD1	*225016_at*	5.2	4.3

Table S2

Primers	*Sequences*	
	Fwd	*Rev*
Lgr5	CTGCCTGCAATCTACAAGGT	CCCTTGGGAATGTATGTCAGA
Survivin	GCCCAGTGTTTCTTCTGCTT	CCGGACGAATGCTTTTTATG
Axin2	CTCCTTATCGTGTGGGCAGT	CTTCATCCTCTCGGATCTGC
Muc2	CGAAACCACGGCCACAACGT	GACCACGGCCCCGTTAAGCA
Krt20	TGTCCTGCAAATTGATAATGCT	AGACGTATTCCTCTCTCACTCTCATA
Fabp2	TGGAAGGTAGACCGGAGT	AGGTCCCCCTGAGTTCAGTT
c-Met	CTGCCTGCAATCTACAAGGT	ATGGTCAGCCTTGTCCCTC
Hgf	CCTATTTCTCGTTGTGAAGGT	TGTTTCGTTTTGGCACAAGA
β-actin	ATGGAAGAAGAGATCGCCGC	TCGTAGATGGGCACCGTGTG